Attitude Estimation
Using Kalman Filtering for Spaceborne SAR Systems

Yongfei Ding[1], Dinghai Xu[1], Yu Li[1], Zheng Fang[1], Tao Chen[1], Hengyang Zhang[2] & Bo Chen[3]

[1]Key Laboratory on Avionics Integration, Aviation Industry of China (AVIC), Shanghai, China
[2]Institute of Navigation and Information, Airforce Engineering University, Shan'xi, China
[3]Institute of Mechanics and Applied Mathematics, Shanghai University, Shanghai, China

Abstract

Doppler parameters of spaceborne Synthetic Aperture Radars (SAR) depend on the orbit elements and the direction of radar antenna pointing. Since satellite attitudes have impact to antenna pointing, accurate estimates of attitude errors are crucial to derive SAR Doppler parameters. To system design perspective, Kalman filtering may continuously track yaw and pitch based on the measurements of Doppler centroid and the information obtained from orbit state vectors. The algorithms being proposed are suitable to both onboard and ground station. We show, by computer simulations, that Kalman filtering may take advantages to provide attitude errors and attitude rates with superior precision. As a consequence, accurate Doppler centroid and Doppler frequency rate may be estimated by explicit calculation from the spacecraft ephemeris.

Keywords: SAR Doppler Parameters, Orbit Elements, Attitude Errors, Kalman Filtering, Turbo Iterations.

1. Introduction

To spaceborne SAR data processing, Doppler parameter estimation [1] is necessary to obtain radar images with satisfied quality. For example, Doppler centroid has to be required by Range Cell Migration Correction (RCMC) and azimuth matched filtering, and Doppler frequency rate has to be accurate enough to focus the images. Imperfect Doppler parameters may lead to the image quality degraded. Two methods are available to achieve Doppler parameter estimation. The first one extracts Doppler parameters from radar echoes. Madsen [2] derived fractional Doppler centroid by using time domain autocorrelation. Cumming [3] and Bamler [4] developed the effective algorithms to resolve Doppler ambiguity. Map drift [5] is probably the most popular algorithm to Doppler frequency rate estimation. However, Doppler parameters obtained by these pioneer works may not be as perfect as expected. These estimation biases are mainly due to unpredictable target characteristics. So, Doppler parameter estimation from radar echoes only may not provide satisfied performance. To the second approach, we may extract Doppler parameters form spacecraft ephemeris. Doppler centroid and Doppler frequency rate can be obtained by explicit calculation based on the Geometric model. Unfortunately, this method also cannot guarantee the precision. To be specific, orbit elements and attitude information provided by spacecraft ephemeris may not as accurate as desired. Attitude errors [6] have significant impacts to Doppler centroid. In addition, such errors can lead to biases to parameters such as effective platform velocity and Doppler frequency rate. As a consequence, the estimator combining the above two methods may be a good choice. Cumming [7] proposed a global surface fit approach to estimate pitch and yaw based on the measurements of estimated baseband Doppler centroid for RADARSAT-1. Furthermore, Wong [8] proposed an algorithm to calculate effective platform velocity with the assumption that prior information of platform attitude and orbit state vectors is available. Their methods can be employed successfully to most practical SAR processors.

To new spaceborne SAR missions, system design may have challenges. Doppler parameter estimation needs the algorithm with better precision and efficiency. In this work, we propose that a Kalman filter could be employed to continuously track attitude information provided that orbit state vectors are known. The spacecraft ephemeris may have guaranteed precision that satisfies the processing requirements.

The paper is organized as follows. In the section 2, we describe the system model. Particularly, the dependence between Doppler parameters and platform attitude errors is derived. In the section 3, we developed the Kalman tracking algorithms to attitude estimation. Both the extended Kalman filter and the iterative Kalman filter are considered. In the section 4, we present the numerical results through computer simulations. The conclusion is drawn in the section 5.

2. System Model

Consider a spaceborne SAR system in the side looking mode. In the Earth Center Inertial (ECI) coordinate, let $\vec{R}_s$ and $\vec{R}_t$ denote the positions of the spacecraft and the target to be illuminated by the radar. It is easy to see that the range between the radar and the target has the form

$$R = \left|\vec{R}_s - \vec{R}_t\right|$$

The Doppler frequency measured at the radar receiver depends on the range rate $\dot{R}$, which is given by Barber in [9]

$$\dot{R} = \dot{R}_s\cos(\gamma) - R_s\omega_s\sin(\gamma)\cos(\psi) + \omega_e R_s\sin(\gamma)[\sin(\psi)\cos(\alpha)\sin(\alpha_i) + \cos(\psi)\cos(\alpha_i)] \quad (1)$$

In the above equation, R_s denotes the range of the satellite, $\dot{R}_s$ denotes its range rate, ω_s represents the angular velocity of the satellite orbit, ω_e represents the angular velocity of earth rotation, α represents the orbit anomaly of the satellite, α_i represents the orbit inclination angle. γ and ψ represent the elevation angle and the direction angle of the radar antenna respectively. $\psi = +\mathrm{pi}/2$ represents right-side looking and $\psi = -\mathrm{pi}/2$ represents left-side looking.

Based on pioneer works [7][9][10], we have developed the geometric model that illustrate the dependence between Doppler frequency and satellite attitudes. In summary, the range rate to a right-side looking radar may be precisely computed as follows

$$A = \dot{R}_s\left[\cos(\theta_{pitch})\cos(\gamma) - \sin(\theta_{pitch})\sin(\gamma)\sin(\theta_{yaw})\right]$$

$$B = R_s\omega_s\left[\sin(\theta_{pitch})\cos(\gamma) + \cos(\theta_{pitch})\sin(\gamma)\sin(\theta_{yaw})\right]$$

$$C = \omega_e R_s\left\{\sin(\gamma)\cos(\theta_{yaw})\cos(\alpha)\sin(a_i) + \left[\sin(\theta_{pitch})\cos(\gamma) + \cos(\theta_{pitch})\sin(\gamma)\sin(\theta_{yaw})\right]\cos(a_i)\right\}$$

$$\dot{R} = A - B + C \quad (2)$$

If the attitudes rotate in the order of yaw=>pitch,

and

$$A = \dot{R}_s\left[\cos(\gamma)\cos(\theta_{pitch})\right]$$

$$B = R_s\omega_s\left[\sin(\gamma)\sin(\theta_{yaw}) - \cos(\gamma)\sin(\theta_{pitch})\cos(\theta_{yaw})\right]$$

$$\begin{aligned} C = \omega_e R_s\{&\left[\sin(\gamma)\sin(\theta_{yaw}) - \cos(\gamma)\sin(\theta_{pitch})\cos(\theta_{yaw})\right]\cos(a_i) \\ &- \left[\sin(\gamma)\cos(\theta_{yaw}) + \cos(\gamma)\sin(\theta_{pitch})\sin(\theta_{yaw})\right]\cos(\alpha)\sin(a_i)\} \end{aligned}$$

$$\dot{R} = A + B - C \quad (3)$$

If the attitudes rotate in the order of pitch=>yaw.

In addition, Doppler frequency rate also depends on orbit elements and radar antenna pointing.

To circular orbits, Raney [10] gave out the closed form result by appropriate approximation,

$$\begin{aligned} R\ddot{R} = {} & R_s\omega_s^2[R_s - R\cos(\gamma)] \\ & -2R_s\omega_e\omega_s\{[R_s - R\cos(\gamma)]\cos(\alpha_i) + R\sin(\gamma)\sin(\psi)\sin(\alpha)\sin(\alpha_i)\} \end{aligned}$$

This result did not consider attitude errors, it may generate unpredictable bias to Doppler parameters.

To make the results less errors, we try to derive an analytic form to Doppler frequency rate incorporating attitude errors. This is the innovation of our work. If the attitudes rotate in the order of yaw=>pitch, the procedures may be summarized as follows

$$A = -\left(\frac{\mu R}{R_s^2}\right)\left[\cos(\theta_{pitch})\cos(\gamma) - \sin(\theta_{pitch})\sin(\gamma)\sin(\theta_{yaw})\right]$$

$$B = \dot{R}_s^2 + R_s^2\omega_s^2$$

$$\begin{aligned} C = {} & R_s^2\omega_s\omega_e\cos(\alpha_i) \\ & -\dot{R}_s R\left[\sin(\theta_{pitch})\cos(\gamma) + \cos(\theta_{pitch})\sin(\gamma)\sin(\theta_{yaw})\right]\omega_e\cos(\alpha_i) \\ & -\dot{R}_s R\left[\sin(\gamma)\cos(\theta_{yaw})\right]\omega_e\cos(\alpha)\sin(\alpha_i) \\ & -R_s R\omega_s\omega_e\cos(\alpha_i)\left[\cos(\theta_{pitch})\cos(\gamma) - \sin(\theta_{pitch})\sin(\gamma)\sin(\theta_{yaw})\right] \\ & +R_s R\omega_s\omega_e\sin(\alpha)\sin(\alpha_i)\sin(\gamma)\cos(\theta_{yaw}) \end{aligned}$$

$$\begin{aligned} D = {} & R_s^2\omega_e^2[\cos^2(\alpha) + \sin^2(\alpha)\cos^2(\alpha_i)] \\ & -R_s R\omega_e^2[\cos^2(\alpha) + \sin^2(\alpha)\cos^2(\alpha_i)]\left[\cos(\theta_{pitch})\cos(\gamma) - \sin(\theta_{pitch})\sin(\gamma)\sin(\theta_{yaw})\right] \\ & +R_s R\omega_e^2[\sin(\alpha)\cos(\alpha) - \cos(\alpha)\sin(\alpha)\cos^2(\alpha_i)]\left[\sin(\theta_{pitch})\cos(\gamma) \right. \\ & \quad \left. + \cos(\theta_{pitch})\sin(\gamma)\sin(\theta_{yaw})\right] \\ & -R_s R\omega_e^2\sin(\alpha_i)\sin(\alpha)\cos(\alpha_i)\sin(\gamma)\cos(\theta_{yaw}) \end{aligned}$$

Where $\mu = 3.986e14$ is the product of the gravitational constant and the mass of earth.

Finally, we have

$$R\ddot{R} = A + B - 2C + D - \dot{R}^2 \tag{4}$$

$$f_R = -\frac{2}{\lambda}\ddot{R}$$

This result can be applied to both circular and elliptic orbits.

3. Kalman Tracking of Platform Attitudes

Obviously, it is very difficult to find yaw and pitch in a closed form. Alternatively, we try to develop the iterative algorithm to tackle this issue.

It is helpful if we define the parameters as

$$\vartheta_{yaw} \triangleq \left[\cos(\theta_{yaw}) \quad \sin(\theta_{yaw})\right]^T$$

and

$$\vartheta_{pitch} \triangleq \left[\cos(\theta_{pitch}) \quad \sin(\theta_{pitch})\right]^T$$

Then the mathematic model being proposed may be represented as

$$\dot{R} = H(\vartheta_{yaw}, \vartheta_{pitch}, \gamma) \tag{5}$$

We might accurately estimate attitude errors by adaptive filters. For example, an LMS adaptive filter or a Kalman filter. By observing Doppler frequency of radar echoes or pilot tone signals, we may continuously track the true attitudes. So, the accuracy of spacecraft ephemeris can be guaranteed.

Let us define the state of the dynamic system

$$x \triangleq \left[\vartheta_{yaw} \quad \dot{\vartheta}_{yaw} \quad \ddot{\vartheta}_{yaw} \quad \vartheta_{pitch} \quad \dot{\vartheta}_{pitch} \quad \ddot{\vartheta}_{pitch}\right]^T \tag{6}$$

This leads to the state equation which can be written as

$$x_{current} = Fx_{previous} + \varepsilon \tag{7}$$

in which F represents the state transition matrix and ε represents the process noise.

Obviously, we have

$$F \triangleq \begin{bmatrix} U & V & W & 0 & 0 & 0 \\ 0 & 0 & 0 & U & V & W \end{bmatrix}^T$$

where

$$U \triangleq \begin{bmatrix} 1 & 0 & T & 0 & T^2/2 & 0 \\ 0 & 1 & 0 & T & 0 & T^2/2 \end{bmatrix}^T$$

$$V \triangleq \begin{bmatrix} 0 & 0 & 1 & 0 & T & 0 \\ 0 & 0 & 0 & 1 & 0 & T \end{bmatrix}^T$$

$$W \triangleq \begin{bmatrix} 0 & 0 & 0 & 0 & 1 & 0 \\ 0 & 0 & 0 & 0 & 0 & 1 \end{bmatrix}^T$$

where T represents the sampling interval along azimuth.

Also, we may write the observation equation as

$$z = H(x, \gamma) + n \tag{8}$$

in which n represents observation noise. This equation leads to a nonlinear mathematical model. Classic Kalman filter cannot be explicitly applied. Fortunately, variants of Kalman filtering may be developed.

3.1 The Extended Kalman Filter

By using first order Taylor expansion, the nonlinear model may be approximated as

$$H(x, \gamma) \approx H(\hat{x}_{pred}, \gamma) + H_e \times (x - \hat{x}_{pred}) \tag{9}$$

where

$$H_e \triangleq \left. \frac{\partial H(x, \gamma)}{\partial x} \right|_{x=\hat{x}_{pred}}$$

Then classic Kalman filtering can be applied, which is summarized as follows

$$\hat{x}_{pred} = F\hat{x}_{previous}$$
$$C_{pred} = FC_{previous}F^T + Q$$
$$\mathrm{Gain} = C_{pred}H_e^T\left(H_eC_{pred}H_e^T + R\right)^{-1}$$
$$\hat{x}_{current} = \pi\left[\hat{x}_{pred} + \mathrm{Gain} \times \left(z - H(\hat{x}_{pred}, \gamma)\right)\right]$$
$$C_{current} = (I - \mathrm{Gain} \times H_e)C_{pred} \tag{10}$$

in which Q represents the covariance of process noise, R represents the covariance of observation noise, and $\pi[\cdot]$ represents the projection operator such that $\|\vartheta_{yaw}\| = 1$ and $\|\vartheta_{pitch}\| = 1$.

It is important to see that the observed Doppler frequency may be in baseband due to PRF ambiguity. In this case, local linearization to the observation equation may not be feasible. Unscented Kalman filter [11] (UKF) may provide a good solution.

3.2 The Iterative Kalman Filter

Further, if we define

$$x_1 \triangleq \begin{bmatrix} \vartheta_{yaw} & \dot{\vartheta}_{yaw} & \ddot{\vartheta}_{yaw} \end{bmatrix}^T \tag{11}$$

and

$$x_2 \triangleq \begin{bmatrix} \vartheta_{pitch} & \dot{\vartheta}_{pitch} & \ddot{\vartheta}_{pitch} \end{bmatrix}^T \tag{12}$$

We may rewrite the observation equation and the state equations

$$z = H(x_1, x_2, \gamma) + n \tag{13}$$

$$x_i^{current} = \tilde{F}x_i^{previous} + \varepsilon_i \qquad \text{For i=1,2} \tag{14}$$

where

$$\tilde{F} \triangleq [U \quad V \quad W]^T$$

It is easy to see that

$$\begin{bmatrix} \hat{x}_1^{pred} \\ \hat{x}_2^{pred} \end{bmatrix} = F\hat{x}_{previous}$$

$$C_i^{pred} = \tilde{F}C_i^{previous}\tilde{F}^T + Q_i$$

$$\mathrm{Gain(i)} = \mathrm{C_i^{pred}} \mathrm{H_i^T} \left(\mathrm{H_i C_i^{pred} H_i^T} + \mathrm{R_i} \right)^{-1}$$

$$\hat{\mathrm{x}}_\mathrm{i}^{\mathrm{current}} = \pi \left[\hat{\mathrm{x}}_\mathrm{i}^{\mathrm{pred}} + \mathrm{Gain(i)} \times \left(\mathrm{z} - \mathrm{H} \left(\hat{\mathrm{x}}_1^{\mathrm{pred}}, \hat{\mathrm{x}}_2^{\mathrm{pred}}, \gamma \right) \right) \right]$$

$$\mathrm{C_i^{current}} = (\mathrm{I} - \mathrm{Gain(i)} \times \mathrm{H_i}) \mathrm{C_i^{pred}} \qquad \text{For i=1,2} \qquad (15)$$

Given the initial values, the Kalman filter may works in a turbo manner [11],

$$\hat{\mathrm{x}}_\mathrm{i}^{(\mathrm{n}-1)} = \hat{\mathrm{x}}_\mathrm{i}^{\mathrm{current}}$$

$$\hat{\mathrm{x}}_1^{(\mathrm{n})} = \pi \left[\hat{\mathrm{x}}_1^{(\mathrm{n}-1)} + \mathrm{Gain(1)} \times \left(\mathrm{z} - \mathrm{H} \left(\hat{\mathrm{x}}_1^{(\mathrm{n}-1)}, \hat{\mathrm{x}}_2^{(\mathrm{n}-1)}, \gamma \right) \right) \right]$$

$$\hat{\mathrm{x}}_2^{(\mathrm{n})} = \pi \left[\hat{\mathrm{x}}_2^{(\mathrm{n}-1)} + \mathrm{Gain(2)} \times \left(\mathrm{z} - \mathrm{H} \left(\hat{\mathrm{x}}_1^{(\mathrm{n})}, \hat{\mathrm{x}}_2^{(\mathrm{n}-1)}, \gamma \right) \right) \right]$$

$$\hat{\mathrm{x}}_\mathrm{i}^{\mathrm{current}} = \hat{\mathrm{x}}_\mathrm{i}^{(\mathrm{n})} \qquad \text{For n=1,2,3,4,5, …} \qquad (16)$$

Notice that, to each iteration, we need update the Kalman gain and the covariance matrixes based on linearization accordingly.

Specifically, we have

$$\mathrm{H}_1^{(\mathrm{n})} = \left. \frac{\partial \mathrm{H}(\mathrm{x}_1, \mathrm{x}_2, \gamma)}{\partial \mathrm{x}_1} \right|_{\mathrm{x}_1 = \hat{\mathrm{x}}_1^{(\mathrm{n})},\ \mathrm{x}_2 = \hat{\mathrm{x}}_2^{(\mathrm{n}-1)}}$$

and

$$\mathrm{H}_2^{(\mathrm{n})} = \left. \frac{\partial \mathrm{H}(\mathrm{x}_1, \mathrm{x}_2, \gamma)}{\partial \mathrm{x}_2} \right|_{\mathrm{x}_2 = \hat{\mathrm{x}}_2^{(\mathrm{n})},\ \mathrm{x}_1 = \hat{\mathrm{x}}_1^{(\mathrm{n})}}$$

4. Numerical Results

Without loss of generality, we employ RADARSAT-1 parameters to computer simulations. Extension to ERS-1 or TerraSAR is also possible. In the Table 1, the parameters used to simulations are listed. As well known, circular orbits have good properties such as simple and efficiency. Due to the characteristics, RADARSAT-1 may take advantages to system design perspective.

In the figure 1-2, we show the effects of attitude errors to Doppler centroid. It is easy to see that both yaw and pitch have impact to Doppler centroid. To look angles less than 45 degrees pitch has more effect than yaw does. This means, in most situations, Doppler centroid is very sensitive to pitch errors. In addition to Doppler centroid, we also need know Doppler frequency rate to SAR data processing. To a perfect situation without attitude errors, the Doppler frequency rate can be plotted as in the figure 3. Also, in the figure 4, we show the errors of Doppler frequency rate due to attitude errors. As can be seen, Doppler frequency rate is not so much sensitive to yaw and pitch, 0.17% error may satisfy the requirements of SAR processing to low resolution images. However, to high resolution processing, these errors have to be considered.

In the figure 5, we show the Doppler centroid variations along both azimuth and range incorporating attitude errors. This surface makes possible that Kalman filtering could generate reliable estimates to yaw and pitch.

Based on the simulated Doppler centroid, the Kalman filters may take advantages to find desired parameters by fast adaptation. In the figure 6-7, we show that the Kalman filter may converge quickly to the pitch and the yaw. In the same way, we obtain the attitude rates, which is shown in the figure 8-9.

Table 1 - System Parameters of RADARSAT-1.

Parameters	Symbols	Values	Metrics
The semi-major axis of the orbit ellipse	a	7167	Kilo-meters
The eccentricity of the orbit ellipse	e	0	NA
The inclination of the orbit plane	a_i	98.6	degrees
The longitude of the ascending node	Ω	0	degrees
The argument of the perigee	ω	NA	degrees
The radar carrier frequency	C	5.3	GHz
The antenna look angle (off nadir)	γ	32, 52	degrees
The average orbit height	H	800	Kilo-meters
Satellite orbit radius	r_s	7189029	meters
Local earth sphere radius	r_e	6390524	meters

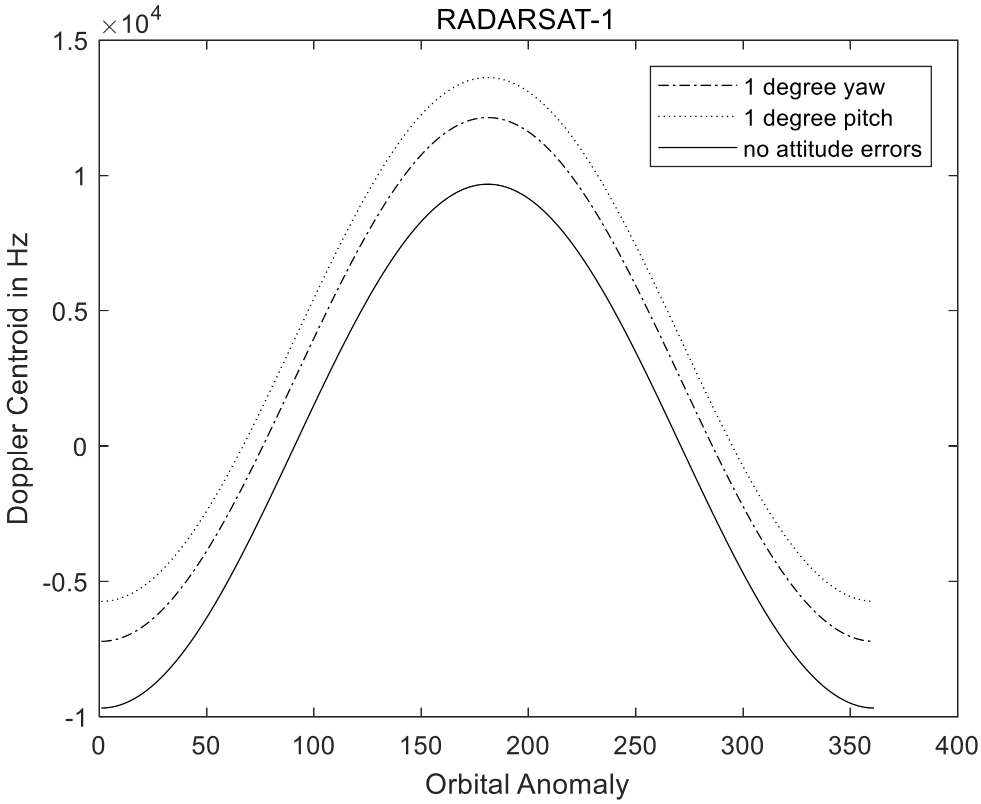

Figure 1 – Effects of Attitude Errors to Doppler Centroid. (look angle = 32 degree)

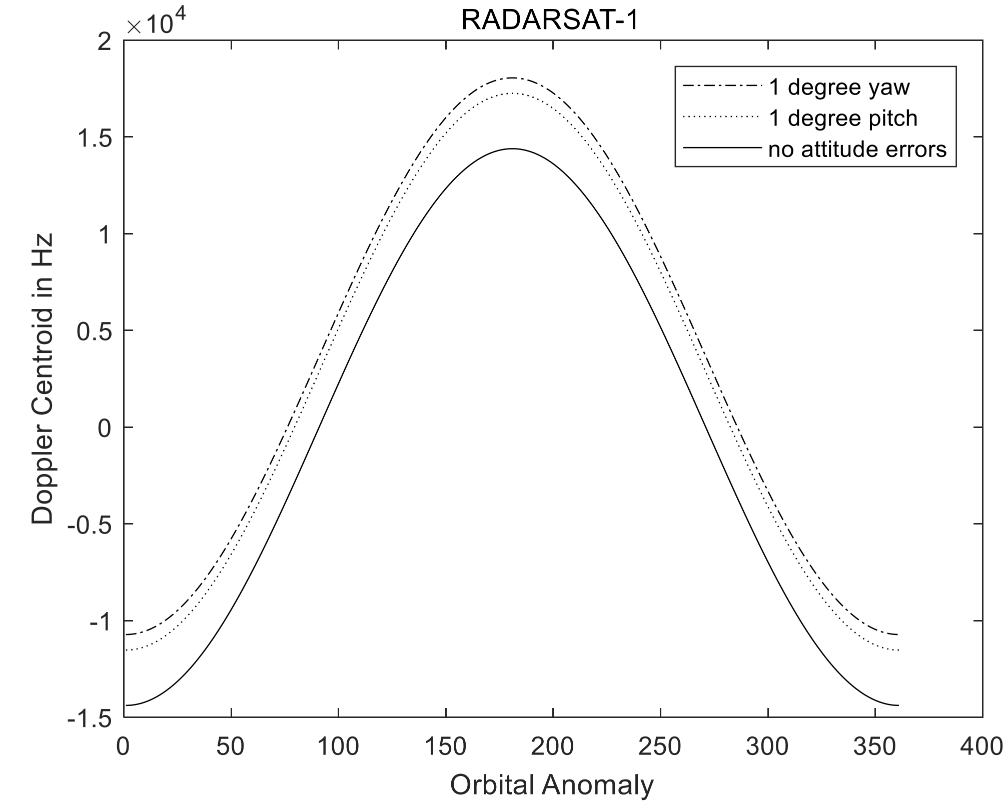

Figure 2 – Effects of Attitude Errors to Doppler Centroid. (look angle = 52 degree)

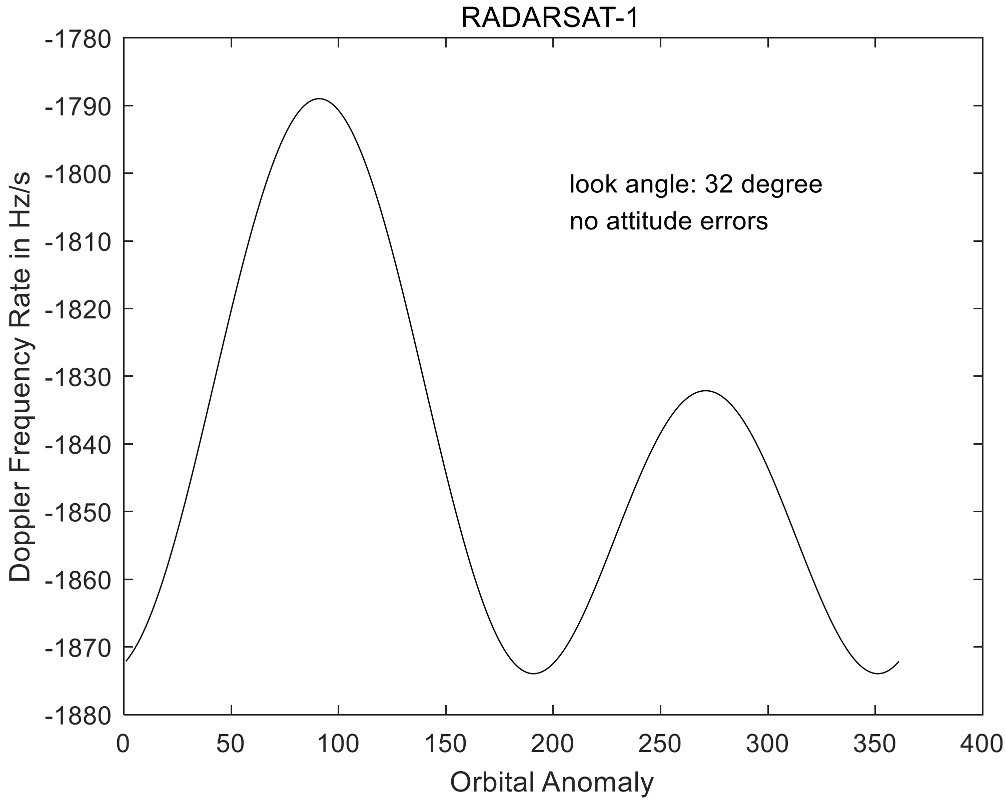

Figure 3 – Doppler Frequency Rate Calculation.

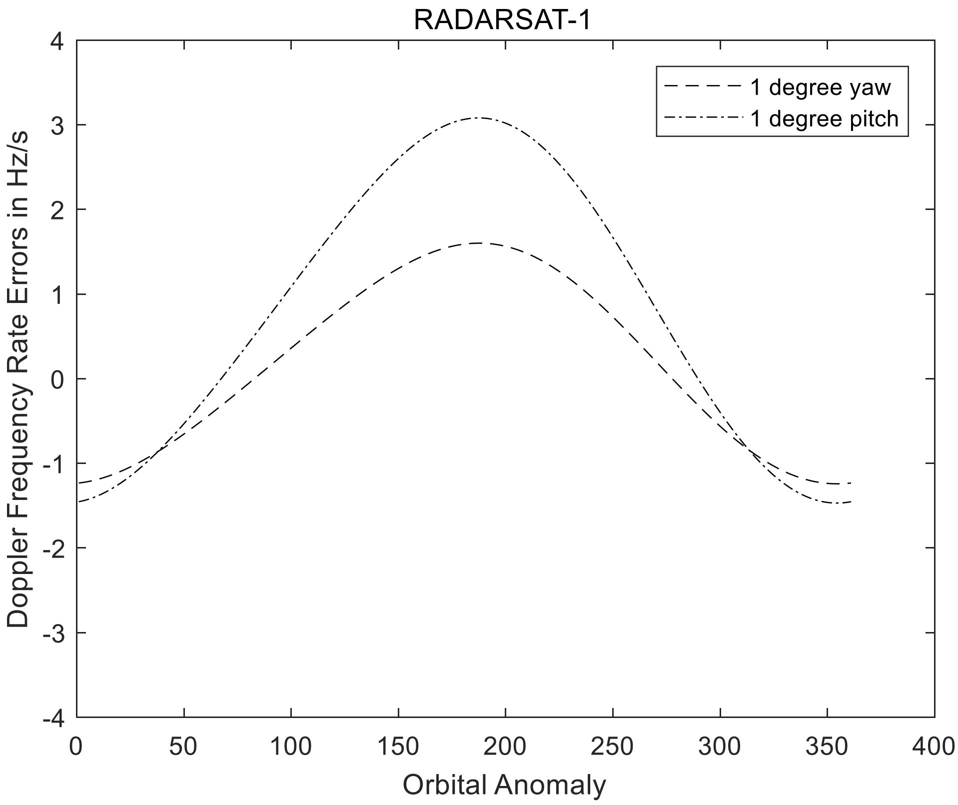

Figure 4 – Effects of Attitude Errors to Doppler Frequency Rate.

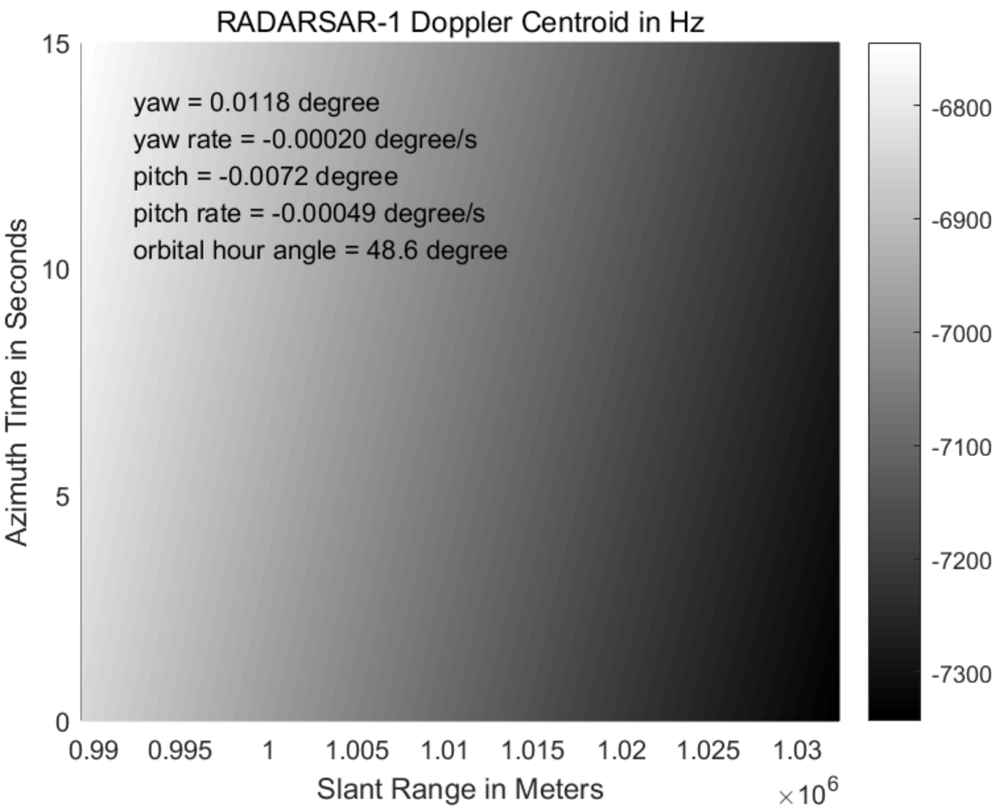

Figure 5 – Effects of Attitude Errors to Doppler Surface.

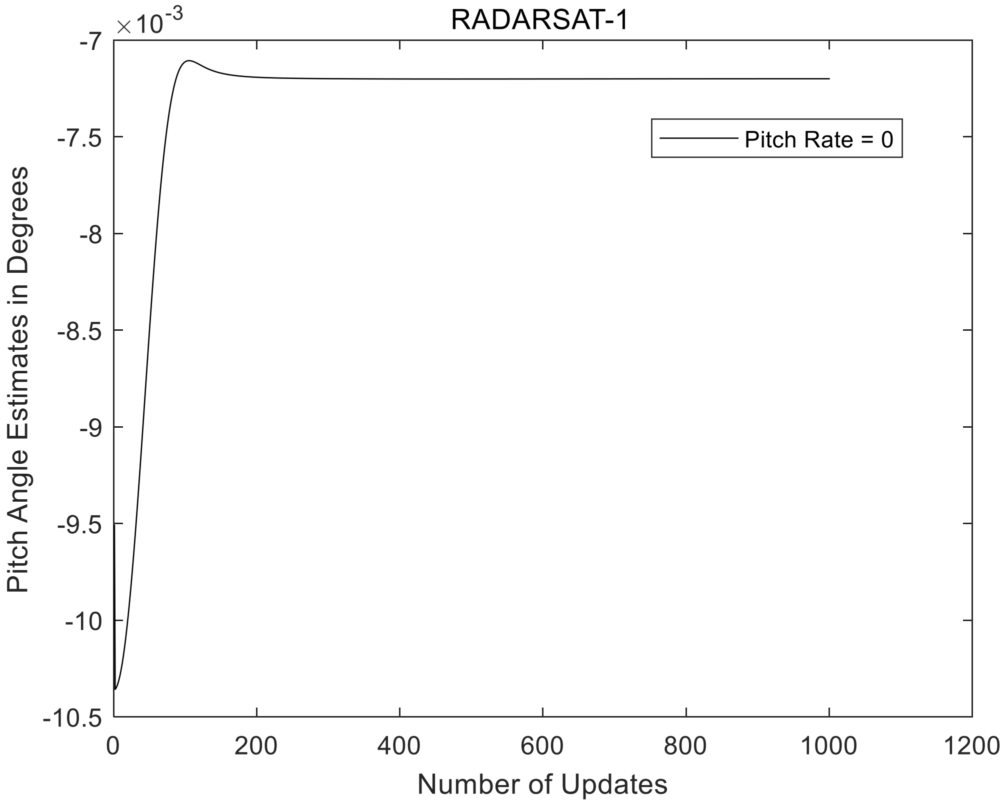

Figure 6 – the Pitch Error by Kalman Tracking.

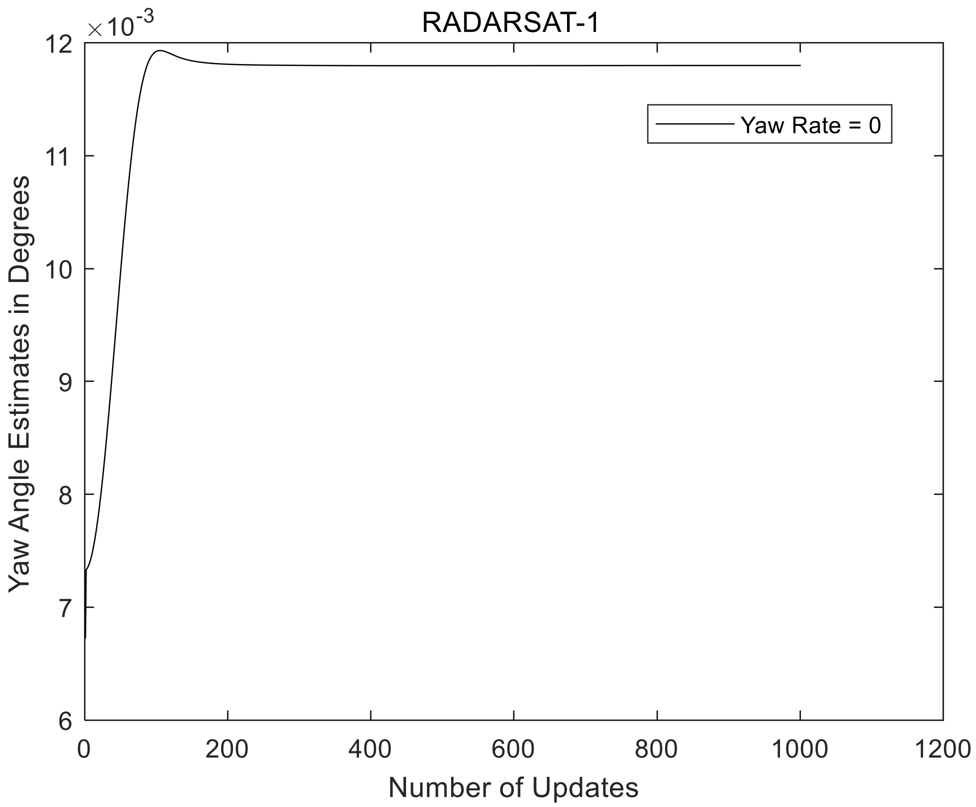

Figure 7 – the Yaw Error by Kalman Tracking.

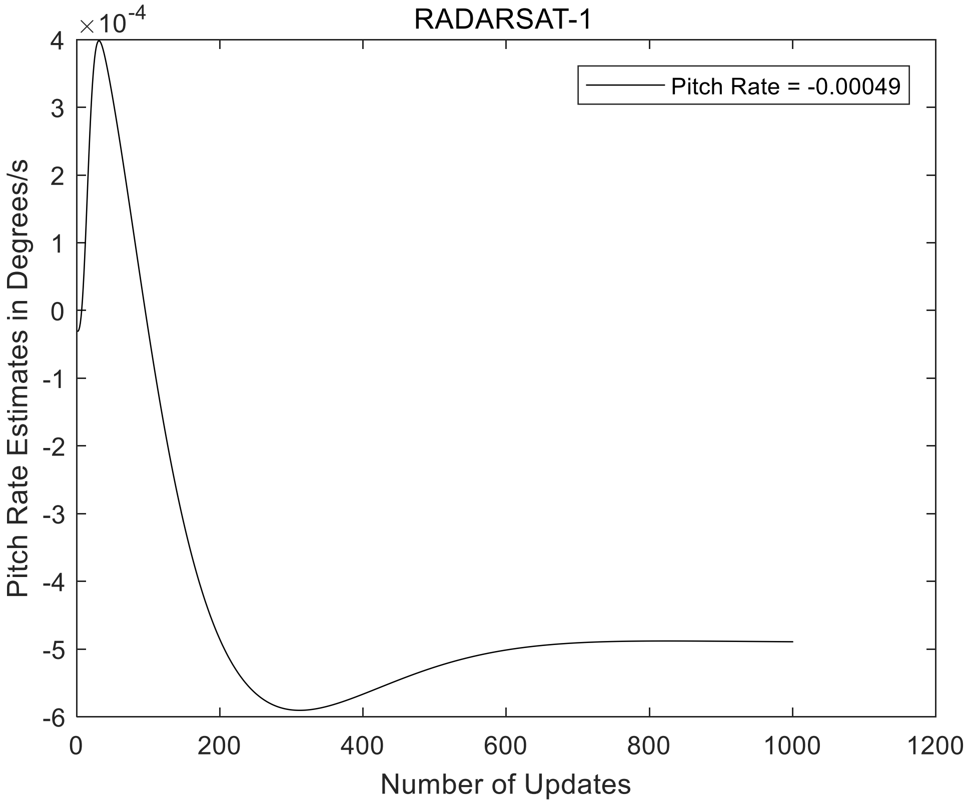

Figure 8 – the Pitch Rate by Kalman Tracking.

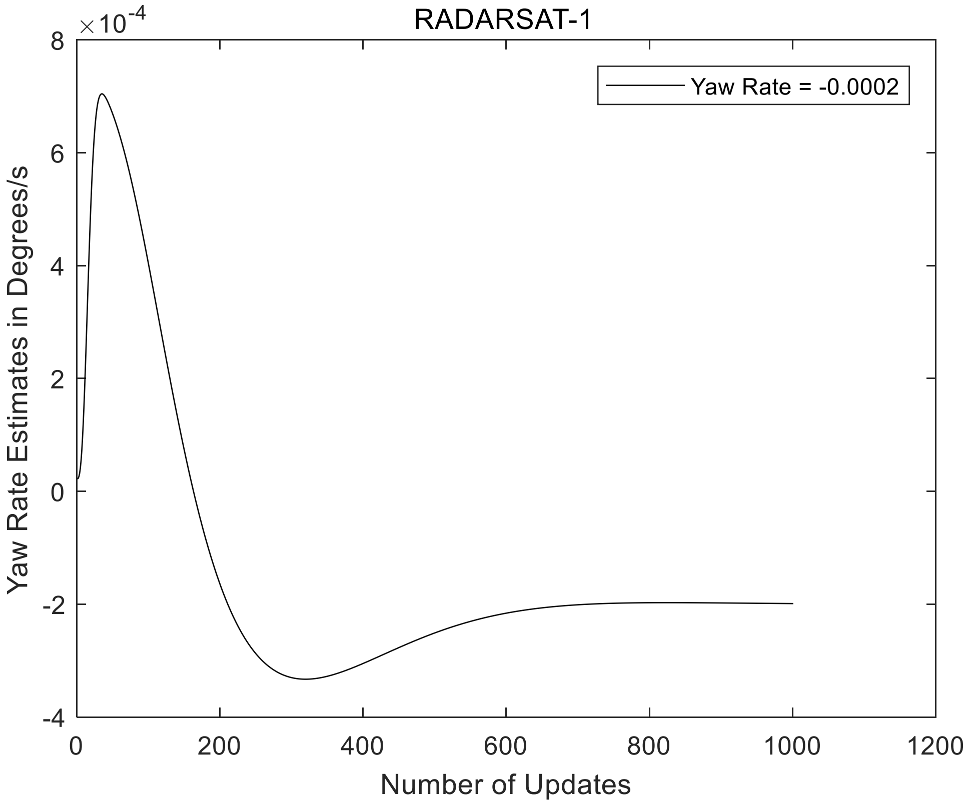

Figure 9 – the Yaw Rate by Kalman Tracking.

5. Conclusions

Kalman filtering is proposed to estimate attitude errors of spaceborne SAR systems. The inputs to the algorithm include radar returns and orbit state vectors. If we assume earth station telemetry could accurately determine orbit elements, Kalman filtering may track attitude errors (yaw and pitch) by measuring unwrapped Doppler frequency. The extended Kalman filter converged quickly to the desired estimates by parameter transform and local linearization. The iterative Kalman filter obtained similar results by parameter separate and turbo iterations. Based on the information of attitude errors, the geometry model may provide more accurate Doppler parameter estimation (Doppler centroid and Doppler frequency rate). This does make sense to a practical SAR processor. Computer simulations demonstrate the superior performance of the Kalman filter based approach. To future investigations, using experiment data to validate the method being proposed needs more efforts. Unscented Kalman filtering may have good performance to wrapped baseband Doppler frequency.

Acknowledgements

This research is supported by Aeronautical Science Foundation (ASF) of China. We would like to appreciate Key Laboratory on Avionics Integration, Aviation Industry of China (AVIC), for the financial and technical supports. Many thanks also go to Institute of Navigation and Information, Airforce Engineering University, for the helpful technical discussion with the distinguished colleagues.

Contact Authors Email Addresses

mailto: dingyf002@avic.com
mailto: xudh007@avic.com
mailto: fangz009@avic.com
mailto: chent080@avic.com
mailto: hareed@163.com
mailto: bochen@shu.edu.cn

Copyright Statement

References

[1] Fuk-Kwok Li, Daniel N. Held, John C. Curlander and Chialin Wu, Doppler Parameter Estimation for Spaceborne Synthetic-Aperture Radars, IEEE Transactions on Geoscience and Remote Sensing, Vol. GE-23, No. 1, pp. 47-56, January 1985.

[2] Soren Norvang Madsen, Estimating the Doppler Centroid of SAR Data, IEEE Transactions on Aerospace and Electronic Systems, Vol. AES-25, No. 2, pp. 134-140, March 1989.

[3] Ian G. Cumming, P. F. Kavanagh, and M. R. Ito, Resolving the Doppler Ambiguity for Spaceborne Synthetic Aperture Radar, in Proceedings of the International Geoscience and Remote Sensing Symposium, IGARSS'86, pp. 1639-1643, Zurich, Switzerland, September 8-11, 1986.

[4] Richard Bamler and Hartmut Runge, PRF Ambiguity Resolving by Wavelength Diversity, in IEEE Transactions on Geoscience and Remote Sensing, Vol. 29, No. 6, November 1991.

[5] Zheng Bao, Mengdao Xing and Tong Wang, Radar Imaging Techniques, in the Chinese language, Publishing House of Electronics Industry, Beijing, 2005.

[6] Hailiang Peng and Donghui Hu, Effect of Satellite Attitude Parameters on SAR Imaging Processing, in the Chinese language, Journal of Electronics, Vol. 15, No. 6, pp. 567-574, November 1993.

[7] Ian G. Cumming, A Spatially Selective Approach to Doppler Estimation for Frame-Based Satellite SAR Processing, in IEEE Transactions on Geoscience and Remote Sensing, pp. 1135-1148, Volume 42, Number 6, June 2004.

[8] Frank H. Wong, Ngee Leng Tan, Tat Soon Yeo, Effective Velocity Estimation for Space-borne SAR, in Proceedings of the International Geoscience and Remote Sensing Symposium, IGARSS'2000, Volume 1, February 2000.

[9] B. C. Barber, Theory of Digital Imaging from Orbital Synthetic-Aperture Radar, International Journal on Remote Sensing, pp. 1009-1057, Volume 6, Number 7, 1985.

[10] R. K. Raney, Doppler Properties of Radars in Circular Orbits, International Journal on Remote Sensing, pp. 1153-1162, Volume 7, Number 9, 1986.

[11] Simon Haykin, Adaptive Filter Theory, the fourth edition, Upper Saddle River, NJ: Prentice Hall, 2002.